

Rotational Ordering Transition in Single-Crystal C₆₀ Studied by Raman Spectroscopy

P. H. M. van Loosdrecht, P. J. M. van Bentum, and G. Meijer

Research Institute of Materials, University of Nijmegen, Toernooiveld, 6525 ED Nijmegen, The Netherlands

(Received 27 November 1991)

Raman spectroscopic data are presented on the rotational ordering fcc → sc transition in single-crystal C₆₀. Splittings and activation of new modes reveal the influence of the cubic structure, and are in agreement with the crystal symmetry in both phases. The temperature dependence of the spectra is consistent with a sharp first-order phase transition near 252 K. A simple model is proposed for the explanation of the temperature dependence of the spectra, involving a large vibrational-rotational coupling in the fcc phase, and essentially no rotational disorder in the sc phase.

PACS numbers: 63.20.Hp, 78.30.Hv, 81.30.Hd

Since the discovery of a new form of carbon, dubbed fullerenes, in 1985 by Kroto *et al.* [1], and the recent development of an efficient method to produce these fullerenes by Krätschmer *et al.* [2], numerous theoretical and experimental investigations have been reported on these exciting new molecules and their derivatives [3–13]. The prototype fullerene is the C₆₀ molecule which has the geometrical structure of a soccer ball with a carbon atom on each of the 60 equivalent corners. It was recently shown by Fleming *et al.* [4] that the truncated icosahedron-shaped C₆₀ molecule crystallizes into a cubic form. X-ray investigations [5] on the structural properties of solid C₆₀ revealed a fcc structure at room temperature, with a (weakly) first-order phase transition [6] to a simple cubic (sc) structure at a temperature near 250 K. The x-ray results, as well as NMR experiments [7,8], show that the fcc → sc phase transition is accompanied by a critical slowing down of the rapid rotations of the C₆₀ molecules.

The vibrational properties of C₆₀ have been studied experimentally by optical spectroscopies [2,9] and inelastic neutron scattering [10], and theoretically by various dynamical calculations [11–13]. A detailed understanding of the vibrational and rotational properties of solid C₆₀ would improve the understanding not only of the C₆₀ solid itself, but also the properties of related compounds such as the high-temperature superconducting alkali-metal-doped fullerenes. In this Letter we present Raman spectroscopic data on the vibrational properties of single-crystal C₆₀, particularly in relation to the fcc → sc phase transition in this material. The sensitivity of optical scattering processes to the crystal field makes Raman spectroscopy, together with infrared spectroscopy, a powerful means to study the solid-state vibrational properties of condensed matter, as well as to detect structural phase transitions.

Unpolarized Raman spectra are recorded in a back-scattering geometry, using a DILOR XY multichannel Raman spectrometer (spectral slit width 3.5 cm⁻¹) with an Ar⁺-ion laser (514.4 nm) as excitation source. The experiments are performed on a sublimation-grown high-purity C₆₀ single crystal [14] (~0.1 mm³). The high quality of the crystals is confirmed by mass spectrometry,

NMR, and electron-diffraction experiments [15]. The crystals thus obtained exhibit natural faces of the {100} and {111} growth forms of the cubic symmetry. The natural faces of the crystal usually show irreproducible Raman intensities when scanned across the surface. Therefore, the crystal is cut along one of the {100} planes, and immediately thereafter mounted on the cold finger of a flow cryostat (temperature stabilization better than 0.5 K, absolute temperature calibration ± 3 K). Subsequently, the cryostat is evacuated to $P \approx 10^{-6}$ mbar. We find that the crystal structure is easily destroyed by intense laser heating due to the strong absorption in the green part of the spectrum, resulting in qualitative changes of the measured Raman spectra. In order to avoid this problem the intensity of the excitation laser is decreased to below 150 μW, focused to a spot of 30 μm. With these precautions the Raman spectra are reproducible for different spot positions on the crystal, and do not depend on the intensity of the excitation laser.

Two representative Raman spectra are displayed in Fig. 1. The upper curve shows the spectrum in the fcc

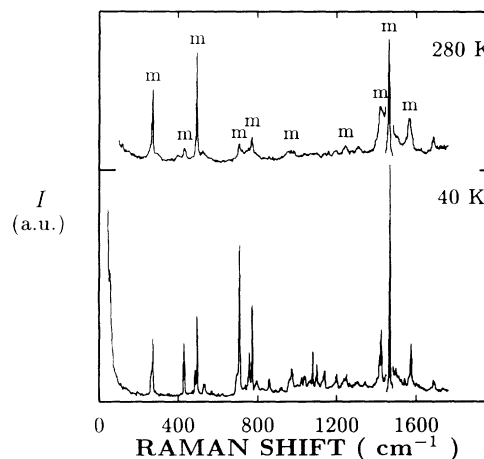


FIG. 1. Unpolarized Raman spectra of single-crystal C₆₀ in the fcc phase ($T=280$ K, upper curve) and in the sc phase ($T=40$ K, lower curve). The peaks at ~ 1467 cm⁻¹ are scaled down by a factor of 6. The predicted modes for the free molecule are indicated with an "m."

phase ($T=280$ K) and the lower curve shows the spectrum for the sc phase ($T=40$ K). The ten modes which are expected purely on the basis of the molecular symmetry are clearly observed in the spectra, though they are generally split up into several lines. Apart from these ten modes, a number of new modes are observed in both spectra. These splittings and the new activated modes can be understood by considering the crystal symmetry of solid C_{60} . The cubic environment of C_{60} in the crystalline state changes the selection rules for optical scattering processes. In the first place, all 23 modes of gerade symmetry will become Raman active in both the fcc and the sc phase, whereas the ungerade modes remain inactive by virtue of the preservation of the inversion symmetry on the sites of the molecules in the crystal. Second, the fourfold- (H_g) and fivefold- (G_g) degenerate modes of the I_h symmetry split up in the fcc phase, and a further splitting of all modes is expected in the sc phase. A factor group analysis based on the T_h site symmetry yields 37 expected Raman-active modes for the fcc phase. For the sc structure which has four molecules per primitive cell and site symmetry S_6 , one finds 145 Raman-active modes. Because of the resolution of the experiment, thermal broadening, and possible (near) degeneracies, one cannot expect to observe all these modes, however. In the fcc phase the spectra exhibit 29 clear peaks and shoulders, whereas in the low-temperature phase we observe 45 modes. The large number of peaks observed in the low-temperature phase is consistent with the sc structure.

Some details of the spectra are shown in Fig. 2, where the upper curves show parts of the spectra in the fcc phase at $T=280$ K and the lower curves show the same region for the sc phase at $T=40$ K. Figure 2(a) shows

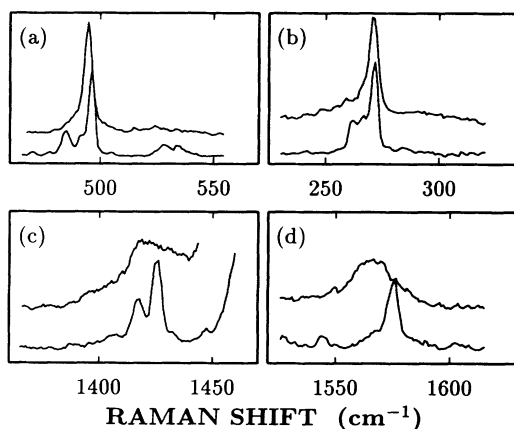


FIG. 2. Parts of the unpolarized Raman spectra of single-crystal C_{60} in the fcc phase ($T=280$ K, upper curves) and in the sc phase ($T=40$ K, lower curves), showing splittings and broadenings for the (a) 496-cm^{-1} A_g , (b) 273-cm^{-1} H_g , (c) 1425-cm^{-1} H_g , and (d) 1575-cm^{-1} H_g regions of the spectra, respectively.

the splitting of the A_g breathing mode in the sc phase. In the high-temperature phase only a single line is expected, which is found at 494 cm^{-1} . In the sc phase, five modes are observed in the displayed region. The strongest peak at 496 cm^{-1} and the shoulder at 493 cm^{-1} can be interpreted as resulting from the $A_g \rightarrow A_g + F_g$ splitting in the sc structure. The strongest mode is the A_g mode, in which the molecules in the primitive cell vibrate in phase, whereas the weaker shoulder at lower frequency can be assigned to the threefold-degenerate F_g mode, corresponding to out-of-phase vibrations of the molecules. The three remaining modes at 485 , 525 , and 533 cm^{-1} correspond to gerade modes which are Raman forbidden for the free C_{60} molecule. They are already weakly, though reproducibly, observed in the high-temperature spectrum.

Figures 2(b), 2(c), and 2(d) show the regions of the 273 -, 1425 -, and 1575-cm^{-1} H_g modes of the molecule, respectively. In the fcc phase, the $H_g \rightarrow E_g + F_g$ splitting is only observable for the 273-cm^{-1} mode, which has a small shoulder on the low-frequency side. The two other H_g modes appear as broad peaks in the spectra. In the low-temperature sc phase, the splitting of the H_g modes is better resolved. In this case, however, one expects eight Raman-active modes per molecular H_g mode according to the $H_g \rightarrow A_g + 2E_g + 5F_g$ splitting. As explained above, one cannot expect to observe all these modes.

Apart from the splittings observed in the spectra, Figs.

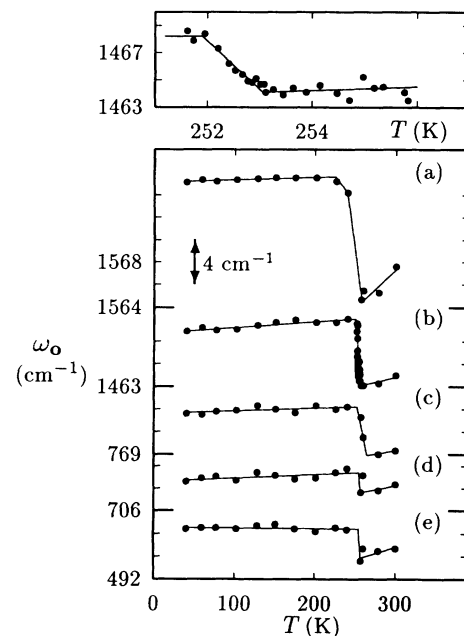


FIG. 3. Temperature dependence of the frequency of the Raman-active modes at (from top to bottom) (a) 1575 cm^{-1} , (b) 1467 cm^{-1} , (c) 772 cm^{-1} , (d) 707 cm^{-1} , and (e) 496 cm^{-1} , respectively. The vertical offset for each curve is indicated by the thick tick marks. Top panel: The 1467-cm^{-1} mode near the fcc \rightarrow sc transition, indicating a discontinuous transition within ~ 1 K. (The solid lines are a guide to the eye.)

1 and 2 also show shifts in frequencies and changes in linewidths of most of the observed modes in the spectra recorded for the two phases. In Figs. 3 and 4 the temperature dependence of the frequency ω_0 and the linewidth Γ [half width at half maximum (HWHM)], respectively, of several of the observed modes are plotted. All frequencies and linewidths plotted in these figures have been determined from spectra taken at a well-stabilized temperature, except for the frequencies of the 1467-cm^{-1} mode between 250 and 255 K. The latter frequencies are determined from spectra recorded while scanning the temperature with $dT/dt \approx -0.06$ K/min. The spectra measured in this temperature interval are integrated over 2 min. The 1467-cm^{-1} mode clearly shows a step in the frequency at the fcc \rightarrow sc phase transition, which is found at $T = 252 \pm 3$ K (see Fig. 3), which agrees well with the results obtained by other authors [5,6]. The width of this steplike behavior of this mode is ~ 1 K, as shown explicitly in the top part of Fig. 3. This discontinuous behavior indicates a first-order character for the phase transition, in agreement with differential scanning calorimetry (DSC) measurements [6] and the discontinuous volume change of about 2.5% found by Heiney *et al.* [5]. For the natural growth faces of the crystal we find a more gradual transition, probably due to surface disorder and/or oxygen adsorption.

For all the modes, a discontinuous behavior is observed in the temperature dependence of the frequency and linewidth. In general, a hardening of the modes of the order of $2\text{--}11\text{ cm}^{-1}$ is observed at the fcc \rightarrow sc phase transition. These hardenings are consistent with the decrease of volume in the sc phase, relative to the fcc phase.

The linewidth of some of the observed peaks plotted in

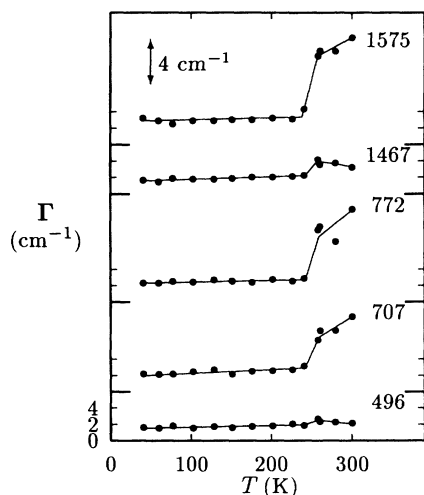


FIG. 4. Temperature dependence of the linewidths of the observed Raman-active modes at (from top to bottom), 1575 , 1467 , 772 , 707 , and 496 cm^{-1} , respectively. The zero point of the vertical scale is indicated for each curve by the thick tick marks. (The solid lines are a guide to the eye.)

Fig. 4 shows a discontinuous decrease at the phase transition. Especially for the 707 -, 772 -, and 1575-cm^{-1} modes, a quite dramatic change by a factor of $3\text{--}4$ is observed. We anticipate that the large linewidths in the fcc phase result from a coupling of these phonons with the rotational motions of the molecules in the fcc phase, effectively decreasing the lifetimes of the phonons, and hence increasing the linewidths of the observed peaks. After prolonged exposure to air or to high laser power, the fcc \rightarrow sc transition becomes less pronounced and appears to shift to lower temperatures. For a clean cleaved surface we find no Raman evidence for a second transition at temperatures below 252 K.

To explain the observed behavior we propose the following simple model. First, at temperatures far above the fcc \rightarrow sc transition we expect the molecules to rotate freely. The intermolecular interactions in the solid give rise to a coupling of the vibrational modes with the quasicontinuum of the rotational excitations, leading to a finite lifetime of these modes. This coupling will be strongest for the modes where neighboring C atoms vibrate out of phase. The coupling to the more symmetric A_g modes is expected to be much smaller, as is indeed the case. Near the transition the rotational motions become strongly hindered, and the molecules now rotate in a hopping-like manner. The hindrance of the rotational motions leads to an increase of the matrix elements representing the rotational-vibrational coupling, but simultaneously result in a decrease of the density of available rotational states. Therefore we expect to observe a decreased linewidth for those modes which already show a strong coupling at temperatures far above the phase transition, and an increase for those modes which do not exhibit this coupling at higher temperatures. This behavior is indeed observed in Fig. 4. In the sc phase the rotational disorder is essentially frozen out. This decreases the linewidth, and only a weak temperature dependence is expected.

For the understanding of the temperature dependence of the frequency of the various modes we consider the main effect to be the volume change near the phase transition. At high temperatures the molecules can be treated as nearly free, held together only by the weak van der Waals forces between the, by virtue of the rotational motions, approximately spherical molecules. The softening of the modes on approaching the transition is not completely understood, but is probably connected with the decrease of the rotational motions. In this regime where the rotations are of a hopping nature one may expect a decrease of the intermolecular potential, provided that the volume does not change dramatically upon approaching the phase transition. At the fcc \rightarrow sc phase transition the modes harden due to the increased interaction potential between neighboring molecules. After the transition no structural changes occur, and the frequency of the modes will be nearly constant in the sc phase.

Apart from the phonons related to the intramolecular vibrations of C_{60} which were considered above, the crystal

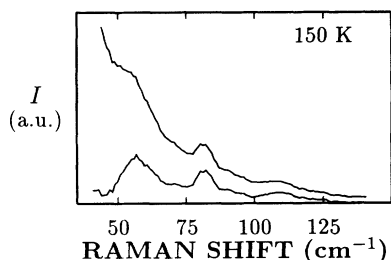


FIG. 5. Part of the unpolarized Raman spectrum at $T=150$ K (upper curve) clearly showing collective lattice modes in the low-frequency region. The lower curve shows the same trace after subtraction of a Lorentzian center peak, revealing three peaks at 56, 81, and 109 cm^{-1} , respectively.

also possesses collective lattice modes, in which the molecules move as a whole. These vibrations can be divided into two classes, one in which the molecules translate, the translational lattice modes, and another class in which the molecules rotate, the librational lattice modes. The first class is of ungerade symmetry for the cubic structure; hence one expects these modes to be only infrared active. The librational modes are of gerade symmetry, and thus are expected to be Raman active (one in the fcc phase and four in the sc phase). Figure 5 shows the low-frequency part of the Raman spectrum at $T=150$ K (upper curve). Clearly this curve shows some structure, which is possibly related to the lattice modes of solid C_{60} . After subtraction of a Lorentzian center peak (Fig. 5, lower curve), the structure appears more clearly as three distinct peaks centered at 56, 81, and 109 cm^{-1} , respectively. These peaks could be due to the librational lattice modes, although one would expect these phonons to have a lower frequency. Therefore the precise assignment of these modes remains unclear.

In summary, we have presented the first detailed temperature-dependent Raman study of a high-purity single-crystal C_{60} . The results show the effects of the fcc and sc crystal structures, both by the appearance of modes corresponding to vibrations which are symmetry forbidden for the molecule, as well as by the observation of a splitting of most of the modes. At the phase transition a discontinuous behavior is observed in the vibration-

al properties of solid C_{60} , with a width of approximately 1 K. The results are explained in terms of a simple model for the crystal. Together with the x-ray [5], NMR [7,8], and DSC [6] results, our results indicate a first-order fcc \rightarrow sc phase transition, in which the rotation of the molecules slows down critically. At variance with the interpretation of the NMR results, we find no rotational disorder in the sc phase. For an understanding of the NMR results, possibly the collective rotational motions in the sc phase have to be taken into account. The Raman spectra reveal three peaks at low frequency, corresponding to collective modes of the crystal. The precise nature of these modes has not yet been revealed.

We gratefully acknowledge the financial support of the Dutch Foundation for Fundamental Research of Matter (FOM).

-
- [1] H. W. Kroto *et al.*, *Nature (London)* **318**, 16 (1985).
 - [2] W. Krätschmer *et al.*, *Nature (London)* **347**, 354 (1991).
 - [3] R. E. Smalley, "The Almost (but Never Quite) Complete Buckminsterfullerene Bibliography" ("Buckybib," available upon request, Dept. of Chemistry, Rice University, P.O. Box 1892, Houston, TX 77251).
 - [4] R. M. Fleming *et al.*, *Mater. Res. Soc. Symp. Proc.* **206**, 691 (1991).
 - [5] P. A. Heiney *et al.*, *Phys. Rev. Lett.* **66**, 2911 (1991); R. Sachidanandam and A. B. Harris, *Phys. Rev. Lett.* **67**, 1467 (1991).
 - [6] A. Dworkin *et al.*, *C. R. Acad. Sci. Ser. B* **9**, 979 (1991). G. Kriza *et al.*, *J. Phys. I (France)* **1**, 1361 (1991).
 - [7] R. D. Johnson *et al.*, *Science* (to be published).
 - [8] R. Tycko *et al.*, *Phys. Rev. Lett.* **67**, 1886 (1991).
 - [9] D. S. Bethune *et al.*, *Chem. Phys. Lett.* **179**, 181 (1990).
 - [10] R. L. Cappeletti *et al.*, *Phys. Rev. Lett.* **66**, 3261 (1991).
 - [11] Z. Slanina *et al.*, *J. Mol. Struct.* **202**, 169 (1989), and references therein.
 - [12] F. Negri, G. Orlandi, and F. Zerbetto, *Chem. Phys. Lett.* **144**, 31 (1988).
 - [13] A. Cheng and M. L. Klein, *J. Phys. Chem.* **95**, 6750 (1991).
 - [14] M. A. Verheijen *et al.*, *Chem. Phys. Lett.* (to be published).
 - [15] G. van Tendeloo *et al.* (unpublished).